Enhancing Retinal Fundus Image Segmentation Using GAN

Manal AlGhamdi

Department of Computer Science and Artificial Intelligence, University of Umm AL-Qura, Makkah, Saudi Arabia

Abstract
Retinal vessel analysis plays a vital role in the detection of some diseases. For example, diabetic retinopathy which may lead to blindness is one of the most common diseases that cause retinal blood vessel structure to change. However, doctors usually take a lot of time and money to collect and label training sets. Thus, automated vessel segmentation as the first step toward computer-aided analysis of fundus remains an active research avenue. We propose an automated Retinal vessel segmentation method based on the GAN network. Traditional image segmentation networks are unsupervised, and GAN is a new semi-supervised network due to adding a Discriminator. By training the discriminator network, we can capture the quality of the generator's output and drive it closer to the true image features. In our experiment, we use DRIVE dataset for training and testing. The final segmentation effect is represented by the Dice coefficient. Experimental results show that the GAN network can effectively improve the edge effect of image segmentation. Compared with the traditional U-net network, GAN shows about 1.55% higher segmentation accuracy.

Keywords:
Retinal image, generative adversarial networks, medical image segmentation.

1. Introduction

The morphological characteristics of fundus images can effectively reflect eye or systemic diseases, such as glaucoma and diabetes because these diseases will affect the retinal morphology to a certain extent, such as the number, branches, width, and angle of fundus vessels [18]. In recent years, many approaches have been proposed to help with the analysis. Among those methods, deep learning algorithms show the best performance with high precision.

Medical datasets often face the following challenges: (1) the number of datasets is insufficient for effective training, (2) for privacy reasons, some real data cannot be used for testing and training, (3) the collection and labeling of training sets usually require a lot of time and money [23, 9]. Therefore, only a tiny portion of annotated medical datasets are available, making them useless for training data-hungry neural networks.

Manuscript received October 5, 2024
Manuscript revised October 20, 2024
https://doi.org/10.22937/IJCSNS.2024.24.10.26

Compared with the previous work of image segmentation using GAN, our contributions are summarized as follows:

- We propose a segmentation method based on a Conditional Generative Adversarial Network (CGAN).
- In our CGAN, the Discriminator discriminates the corresponding region patches of every pair of images, and the size of every patch is 1×16×16, which is different from the traditional method of distinguishing complete images. This rule is more conducive to improving the quality of real information carried by the generated images, which are also the segmentation results.

2. Related Work

Our tasks mainly include the construction of a segmented network and the training of CGAN. Here, we will separately describe the representative work of these two tasks.

a. Retinal Fundus Image Segmentation

In clinical medicine, doctors need to observe and manually label color fundus images, but pixel-level manual annotation is a costly and time-consuming process. Therefore, the realization of the intelligent segmentation of fundus blood vessels has a strong research significance.
Automated segmentation of blood vessels from a fundus image is challenging due to intricate branching patterns, a noisy background, and illumination differences.

In a few years, many ways have been raised to solve this problem [9]. Such as unsupervised methods: Threshold segmentation, Region Growing, Gray Level Co-occurrence Matrix, Local Adaptive

Threshold, Morphological Operations, Otsu thresholding, and Template Matching [28, 30, 29].
As an important research field of pattern recognition and machine learning, supervised learning has made great progress in theory and application. At the same time, based on the maturity of artificial neural networks, people try to apply it to fundus vascular segmentation. Such as Linear Discriminant classifiers, Support Vector, Machine (SVM), Naive Bayes classifier, Random Forest algorithm [6, 16].
The development of Convolution Neural Network (CNN) further promotes the quality of retinal vessel segmentation [5, 24, 19]. To enhance the segmentation effect of small vessels, researchers try to combine CNN with other algorithms to optimize the segmentation quality. For example, a dense conditional random field (CRF) model has been successfully used in final vessel segmentation [31]. However, the blood vessels segmented by the above methods are quite blurry, and errors often appear at the end of branches.

In the current biomedical image segmentation tasks, the U-net structure is the most used segmentation method. Compared with the previous methods, it shows good segmentation characteristics [22, 15]. Based on the traditional u-net, many more advanced u-net networks have been proposed. A deformable U-net (DUnet), with up-sampling operators to increase the output resolution, is designed to extract context information and enable precise localization by combining low-level features with high-level ones [12]. To solve the defects of the global-based method in dealing with details, a Global and Local enhanced residual U-net (GLUE) for accurate retinal vessel segmentation benefits from both the globally and locally enhanced information inside the retinal region [13]. In our GAN, U-net featuring Encoder-Decoder architecture with skip connection is used as a generator.

b. Generative Adversarial Network

Generative Adversarial Network (GAN) was first proposed by Goodfellow in 2014 [8]. GAN consists of a Generation network and a Discriminant network. These two networks become stronger at the same time through confrontation training. Through the mutual game of two neural networks, the Generator finally generates an output whose distribution is very close to

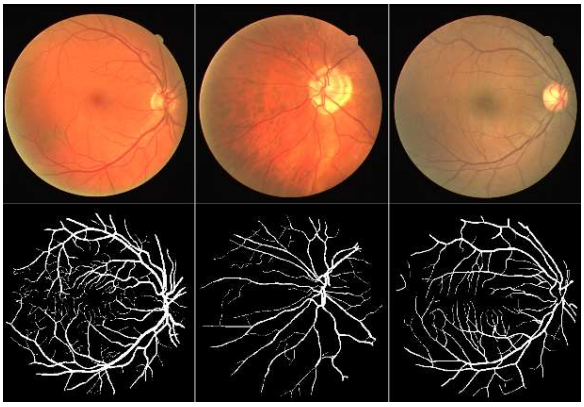

Fig. 1. Examples from the DRIVE dataset

the real data distribution. This semi-supervised learning method shows strong advantages in image processing tasks so that GAN has been extensively applied in data augmentation [4], image classification, and virtual image generation. Compared with other generation models, Gan can produce better-generated samples based on actual results. However, there are many problems with the original GAN. Training GAN needs to reach the Nash equilibrium, and the training GAN model is unstable. Besides, it is difficult to learn to generate discrete data. To achieve “victory”, the generator will choose the samples that are easy to generate.

Later, many optimized structures that are based on GAN are proposed, such as Deep Convolutional GAN (DC- GAN) [21], Conditional GAN (CGAN) [11], Wasserstein GAN (WGAN) [1] and Least-Square GAN (LSGAN) [17]. We use CGAN in this project. The optimization process of CGAN is similar to that of GAN. The difference is that random noise and additional conditions are used as inputs of this artificial neural network. Through this method, CGAN can add conditions to the original GAN to guide the data generation process so as to generate samples with specific properties.

3. Data

The first task of the experiment is to obtain the data. By searching for relevant resources, we found that DRIVE [27], Chase DB [20], and STARE [10]are high-quality datasets for retinopathy studies. We decided to use the DRIVE dataset, which has related images from the diabetic retinopathy screening

program in the Netherlands. There are 400 people aged between 25 and 90 years old, but only 40 fundus

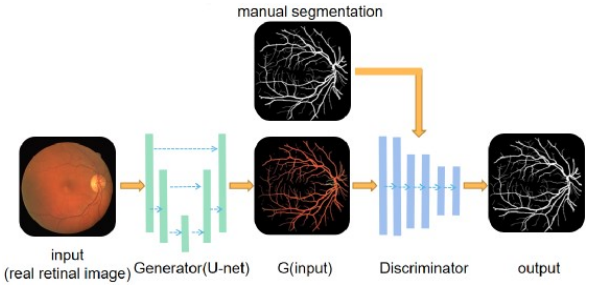

Fig. 2. The architecture of our network

images were randomly selected, of which 33 were normal. Seven of the fundus images showed traces of mild early diabetic retinopathy. The 40 images in DRIVE dataset were divided into two parts, which were used as a training set and a test set. Figure 1 shows an example from this dataset.

4. Methodology

Here, we will introduce the structure of the neural network we use. We will then describe in detail the principles and applications of U-net and CGAN. Finally, we will explain the details of the implementation of the whole architecture.

c. Network Architecture

The overall architecture we built and trained is shown in Figure 2. In our architecture, the real color fundus images are used as the inputs of U-net, and the outputs are considered the initial fundus segmentation images. It should be noted that we also use U-net as the Generator of CGAN. Therefore, these initial fundus segmentation images will then be judged by the CGAN discriminator, which will make them more closely related to the features of the real fundus images. Finally, through the supervision of the Discriminator, the segmentation accuracy of small blood vessels will be improved.

d. U-net

At present, the best network structure in the field of fundus vascular segmentation is based on the improved version of the original U-net. U-net was proposed by Olaf [2] to be used for cell segmentation in medical images.

U-net is a perfectly symmetrical structure consisting of three parts: a contraction path, an expansion path, and a jump connection [14] as shown in Figure 3. The contraction path is mainly used to extract useful features from the image.

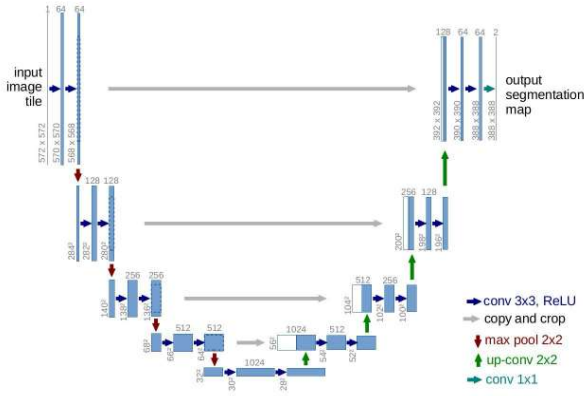

Fig. 3. The implementation process of U-net

The composition structure is mainly to carry out two convolution operations on the input image. After every convolution, there is an activation function. The convolution kernel uses the convolution kernel with a size of 3×3, and the input feature map uses padding operation. The padding value is 1, and the convolution step size is 1, the activation function is ReLu activation function, so the size of the feature map obtained is the same as that of the input feature map. The kernel size is 2×2, and the step size is 2. A feature graph with length and width half of the input feature map is output. The number of channels in the characteristic graph increases exponentially except that the first layer is changed from 1 channel to 64 channels. Repeat this structure four times to get a characteristic graph with 512 channels, and use 3×3 convolutions to get a characteristic graph with 1024 channels.

The next operation is to reduce the number of channels and increase the length and width of the characteristic graph. This part belongs to the expansion path. First, the characteristic graph with 1024 channels is convoluted by 3×3, and then four repeated expansion structures are followed. A deconvert convolution kernel is 3×3, and the step size is 2. A feature whose length and width are increased by twice and the number of channels is reduced by half is obtained. These feature graphs are connected with the feature graphs copied from the contraction path according to the channel dimension. This operation is

a jump connection. After two 3×3 convolutions, the feature graph padding is 1, the convolution step is 1 and the activation function is ReLu. After the first convolution, the number of channels is reduced by

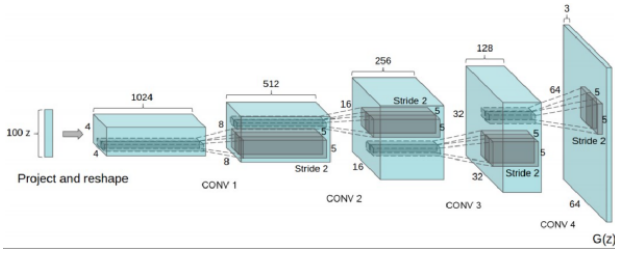

Fig. 4. The internal structure of GAN

half, and the final result is obtained when the length and width are increased by two and the number of channels becomes half of the original. Repeat four times to get a feature map of multiple channels with the same size as the original image. Finally, through a 1×1 convolution operation, an image with 1 channel is obtained, and the output size is the same as the original image. In this way, a pixel- to-pixel task is completed.

In our experiment, we build a U-net based on the above theory. On the one hand, we record the segmentation outputs of U-net and train the U-net as the generator of GAN and record the generated results of GAN. By comparing the Dice coefficients of these two segmentation images, we find that GAN can effectively enhance the segmentation effect.

e. Conditional Generative Adversarial Network (CGAN)

In this paper, we use CGAN [1] to improve the image quality of fundus vascular segmentation. The optimization objective function of the original GAN can be expressed as:

$$\min_G \max_D V(D,G) = E_{x\ Pdatax}[log(D(x))] + E_{z\ P_z(z)}[log(1 - D(G(z))] \quad (1)$$

As shown in Figure 4, the input of GAN is random noise which is the noise randomly sampled from a distribution. The generator takes the noise as input and produces a false distribution. Then, a true distribution that we want to obtain, and a false distribution produced by the generator will be passed to the discriminator. The task of the discriminator is to judge the generated distribution as false and the real distribution as true [25].

When training Discriminator, maximize formula (1) and train Generator, minimize formula (1). In fact, Generator is responsible for mapping data from a certain part of the space to a low dimensional manifold in a high-dimensional space, while Discriminator is responsible for drawing the generated manifold space closer to the real distribution. In this process, the game between Generator and Discriminator is formed and the performance of both neural networks will be improved. Finally, it can achieve the goal that the Discriminator can not distinguish the output of the Generator and the real distribution, which shows that the image generated by GAN has the characteristics of real distribution to a great extent.

The key to improving the performance of GAN is to establish a suitable loss function, which can make GAN easier to train. Therefore, based on the original GAN, many derived neural networks are constructed. CGAN is one of them.

The CGAN adds conditions as control instructions on the basis of GAN. We define the real fundus image as Y and the real vascular image as X. The objective of CGAN can be expressed as:

$$L_{GAN} = \min\max E_{x\ Pdatax}[log(D(x,y))] + E_{z\ Pdataz}[log(1 - D(G(z,y),y))] \quad (2)$$

$$L_{L_1} = E_{x,y\ Pdata(x,y)}[||G(x,y) - x||] \quad (3)$$

where

$$(x_i)_{i=1}^{n}\ 2\ X,\ \ (y_i)_{i=1}^{n}\ 2\ Y$$

Our total objective is:

$$L_{CGAN} = L_{CGAN} + \lambda L_{L1} \quad (4)$$

Where λ balance two objective functions.

f. Implementation Details

In the process of configuring the loss functions of Generator and Discriminator, we use Mean Square Error (MSE) and Mean Absolute Error (MAE) as the loss function. Their specific mathematical expressions are:

$$MSE = \frac{1}{n}\sum_{i=1}^{n}(y_i - \hat{y}_i)^2 \quad (5)$$

$$MAE = \frac{1}{n}\sum_{i=1}^{n}|y_i - \hat{y}_i| \quad (6)$$

where n is the number of samples.

In fact, MAE is more robust to outliers, but its derivative discontinuity makes the process of finding the optimal solution inefficient; MSE is sensitive to outliers, but it is more stable and accurate in the optimization process. In addition, MAE is also called L1 loss.

We initialize the parameters of the whole net using random numbers from a normal distribution. To be more specific, N(0, 0.02) for convolutional layers, and N(1, 0.02) for batch normalizing layers. We use Adam solver with a fixed learning rate of 0.0002, and set β1 = 0.5, β2 = 0.999. The optimizer employed is Adam, which can be expressed as:

$$m_t = b_1 m_{t-1} + (1 - b_1)dx \quad (7)$$

$$v_t = b_2 v_{t-1} + (1 - b_2)dx^2 \quad (8)$$

$$W_t = W_{t-1} - \frac{\lambda m}{\sqrt{v}} \quad (9)$$

where λ is the learning rate. In our program, the learning rate is 0.0002

Notice that the segmented results are black and white images, a hyperbolic function, which is added in the end of generator models as tanh, is the key to the training. Without this activation function, the segmented vessels will likely decrease the brightness in some epochs and finally fall into a situation where only black images are generated. It has a high incidence rate; in our experiment, without the hyperbolic function, neither the generator is implemented with U-net, nested U-net, or modified Resnet34 faces this kind of failure after hundreds of epochs.

5. Experiments

Our experimental process mainly includes the following steps: 1. Data preprocessing. 2. Train the U-net network to get segmented images. 3. Build and train the CGAN network to get segmented images. 4. Evaluate the segmentation results of CGAN based on the Dice coefficient. Next, we will introduce the above four links.

a. Data Preprocessing

Before the development of deep learning technology, more complex image preprocessing is needed. Because of various imaging conditions, such as noise, uneven light intensity, poor visibility of thin vascular

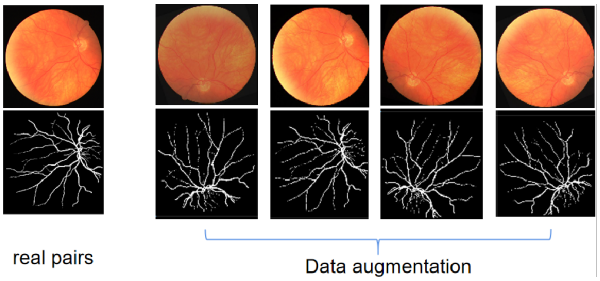

Fig. 5. Data augmentation(methods:random zoom, random ro- tation, brightness swift and contrast swift)

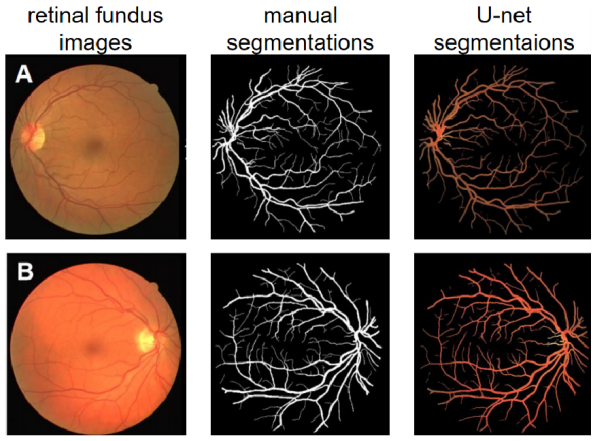

Fig. 6. Outputs of U-net

structure, anatomical variation, and other imaging artifacts, vascular segmentation is very difficult. Therefore, pretreatment steps are needed to improve the segmentation accuracy before any vessel segmentation. At present, the main preprocessing methods [26] include removal of central vascular reflex [7], correction of uneven strength, and vascular enhancement [3]. It is worth noting that due to the defects of the algorithm itself, these methods are not necessarily conducive to improve the quality of subsequent segmentation in the process of practice.

The development of deep learning algorithm solves the problem of improving segmentation quality. Under the method of supervised learning, a large number of labeled data are needed. Therefore, in our experiment, the data process mainly includes data expansion and image size standardization. Due to the small amount of raw data provided by the DRIVE dataset, we utilize preprocessing methods such as zoom, rotation, and horizontal flip change to augment the image pairs. Besides, the brightness value and contrast value of fundus pictures are also changed randomly. The augmentation is parallel for both raw images and manual segmentation with the same random seed employed.

b. Segmentation results of U-net

Initially, we used U-net with pooling layers and basic long skip connections to generate the segmented results. In the very beginning of training U-net, we didn't make data augmentaion. Training With 1700 epochs where each epoch has 20 pairs of fixed images, the network shows an accuracy rate with *Dice* coefficient as 66.73% on the test dataset in *DRIVE*.

Then, we made an augmentation module on the former U-net, which means that the image pairs here have already been augmented through the same methods mentioned in Figure 5. Here, the value of *Dice* coefficient rises to75.93% We present the results of U-net in Figure 6. According to this result, we can conclude that data augmentation can fairly improve the quality of segmented images.

c. Segmentation results of CGAN

To build our CGAN, A discriminator, which is composed of convolutional layers and Leaky ReLU activation functions are added into training.

We configure the appropriate initialization weight, the loss function of the two neural networks, and the optimizer.

In particular, we use U-net in the previous step as Genera- tor of CGAN and its segmented images will then be judged by the Discriminator according to every patch with a size of 1×16×16. The Dice coefficient is lifted to 77.48% after 1700 epochs. The outputs of our CGAN are shown in Figure 7.

Improving the segmentation quality of U-net is an important link to improve CGAN. We have made some attempts and improvements. We also tried to adjust Resnet32 into a generator. It should have brought us another contribution, while the Dice coefficient kept floating around 61.30%.

The Nested U-net is another choice of generator, where the network has hidden blocks, which link the nearest blocks. According to this architecture, the demand of memory increases dramatically with the growth of the depth of the network. Limited by the device we have, a 4L nested U-net is trained, showing a Dice of 35.03% after 1500 epochs.

Although the training result is not satisfying, it should improve the result if we can allocate more resources.

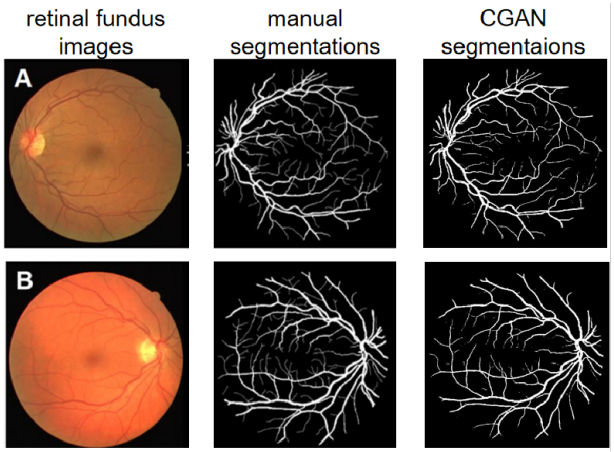

Fig. 7. Outputs of CGAN

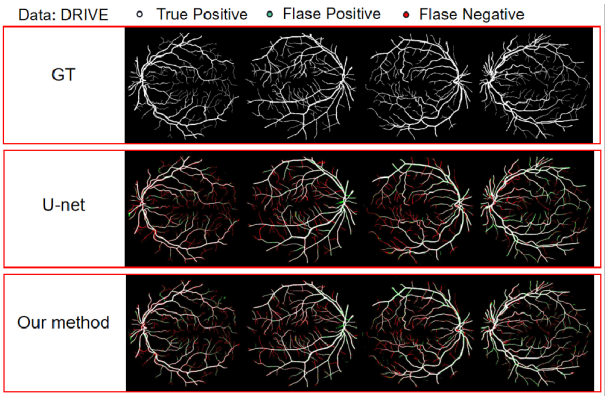

Fig. 8. The figure shows the ground truth of segmentation, the results of U-net segmentation and the results of our approach;each column corresponds to the same retinal fundus image.

Table 1: Segmentation quantiative evaluation with Dice.

Method	Dice
U-net without augmentation	66.73%
U-net	75.93%
Ours	77.48%

In the process of our experiments, We observed that generators with skip connections, especially those keep short and long skip connections with them, have a tend to start with many segmented vessels both thick and interconnected. In the contrast, with few skip connection, the result will start with separated few vessels segmented after the initial chaos. As for learning rate, 0.0002 is a common choice, which is mentioned by many authors in their papers. Once the learning rate is set too small, like 0.00002, it will be hard to reach a convergence, and the parameters are likely to be trapped in a locally optimal condition, causing failure.

d. Results Evaluation

Figure 8 shows the segmentation results of U-net and the results of our CGAN. Observing the segmented image directly, we can see that the segmentation accuracy of CGAN in small vessels is higher than that of U-net. Specifically, the segmentation results of CGAN can better reflect the small branches of blood vessels.

We unifiedly use Dice coefficient to quantify the segmentation quality of these two methods and the results are shown in Table 1. This result shows that compared with the traditional U-net, our CGAN can improve Dice coefficient by about 1.55%. This means that our method can more effectively realize the fundus vascular segmentation.

6. Conclusions and Discussions

In this paper, we introduce a CGAN framework for retinal fundus segmentation based on condition GAN. Compared with the traditional U-net, which is the most popular vascular segmentation method nowadays, Our CGAN performs better in Dice coefficient. The results of our experiments show that our method can be more effectively applied to the field of medical image segmentation, such as fundus blood vessel segmentation.

However, by observing the segmentation results of CGAN, we find that although the segmentation image performs better on thin blood vessels, there will be false points that are inconsistent with the real fundus vascular characteristics at the edge of the segmented images. This is not conducive to practical clinical application. This problem is related to the principle of GAN itself and we think it can be corrected by optimizing the structure of U-net. We consider this point as the main defect of our current work and it is also where we plan to improve in our future work.

References

[1] M. Arjovsky, S. Chintala, and L. Bottou. Wasserstein gan, 2017.

[2] G. Azzopardi, N. Strisciuglio, M. Vento, and N. Petkov. Trainable cosfire filters for vessel delineation with application to retinal images. Medical image analysis, 19(1):46–57, 2015.

[3] P. Bankhead, C. N. Scholfield, J. G. McGeown, and T. M. Curtis. Fast retinal vessel detection and measurement using wavelets and edge location refinement. PloS one, 7(3):e32435, 2012.

[4] C. Bowles, L. Chen, R. Guerrero, P. Bentley, R. Gunn, A.Hammers,D.A.Dickie,M.V.Herna´ndez,J.Wardlaw, and D. Rueckert. Gan augmentation: Augmenting training data using generative adversarial networks. arXiv preprint arXiv:1810.10863, 2018.

[5] P. Chudzik, B. Al-Diri, F. Caliva´, and A. Hunter. Discern: Generative framework for vessel segmentation using convolutional neural network and visual codebook. In 2018 40th Annual International Conference of the IEEE Engineering in Medicine and Biology Society (EMBC), pages 5934–5937. IEEE, 2018.

[6] M. Fraz, P. Remagnino, A. Hoppe, and S. Barman. Retinal image analysis aimed at extraction of vascular structure using linear discriminant classifier. In 2013 International Conference on Computer Medical Applications (ICCMA), pages 1–6. IEEE, 2013.

[7] M. M. Fraz, A. R. Rudnicka, C. G. Owen, and S. A. Barman. Delineation of blood vessels in pediatric retinal images using decision trees-based ensemble classification. International journal of computer assisted radiology and surgery, 9(5):795–811, 2014.

[8] I. Goodfellow, J. Pouget-Abadie, M. Mirza, B. Xu, D. Warde-Farley, S. Ozair, A. Courville, and Y. Bengio. Generative adversarial nets. In Advances in neural information processing systems, pages 2672–2680, 2014.

[9] G. HaoQi and K. Ogawara. Cgan-based synthetic medical image augmentation between retinal fundus images and vessel segmented images. In 2020 5th

International Conference on Control and Robotics Engineering (ICCRE), pages 218– 223. IEEE, 2022.
[10] A. Hoover, V. Kouznetsova, and M. Goldbaum. Locating blood vessels in retinal images by piecewise threshold probing of a matched filter response. IEEE Transactions on Medical imaging, 19(3):203–210, 2000.
[11] P. Isola, J.-Y. Zhu, T. Zhou, and A. A. Efros. Image-to-image translation with conditional adversarial networks. In Proceedings of the IEEE conference on computer vision and pattern recognition, pages 1125–1134, 2017.
[12] Q. Jin, Z. Meng, T. D. Pham, Q. Chen, L. Wei, and R. Su. Dunet: A deformable network for retinal vessel segmentation. Knowledge-Based Systems, 178:149–162, 2019.
[13] S. Lian, L. Li, G. Lian, X. Xiao, Z. Luo, and S. Li. A global and local enhanced residual u-net for accurate retinal vessel segmentation. IEEE/ACM transactions on computational biology and bioinformatics, 2019.
[14] J. Long, E. Shelhamer, and T. Darrell. Fully convolutional networks for semantic segmentation. In Proceedings of the IEEE conference on computer vision and pattern recognition, pages 3431–3440, 2015.
[15] L. Luo, D. Chen, and D. Xue. Retinal blood vessels semantic segmentation method based on modified u-net. In 2018 Chinese Control And Decision Conference (CCDC), pages 1892–1895. IEEE, 2018.
[16] D. Mahapatra and J. M. Buhmann. Obtaining consensus annotations for retinal image segmentation using random forest and graph cuts. 2015.
[17] X. Mao, Q. Li, H. Xie, R. Y. K. Lau, Z. Wang, and S. P. Smolley. Least squares generative adversarial networks, 2016.
[18] A. T. Nair and K. Muthuvel. Blood vessel segmentation and diabetic retinopathy recognition: an intelligent approach. Computer Methods in Biomechanics and Biomedical Engineering: Imaging & Visualization, 8(2):169–181, 2020.
[19] A. Oliveira, S. Pereira, and C. A. Silva. Retinal vessel segmentation based on fully convolutional neural networks. Expert Systems with Applications, 112:229–242, 2018.
[20] C. G. Owen, A. R. Rudnicka, R. Mullen, S. A. Barman, D. Monekosso, P. H. Whincup, J. Ng, and C. Paterson. Measuring retinal vessel tortuosity in 10-year-old children: validation of the computer-assisted image analysis of the retina (caiar) program. Investigative ophthalmology & visual science, 50(5):2004–2010, 2009.
[21] A. Radford, L. Metz, and S. Chintala. Unsupervised representation learning with deep convolutional generative adversarial networks. arXiv preprint arXiv:1511.06434, 2015.
[22] O. Ronneberger, P. Fischer, and T. Brox. U-net: Convolutional networks for biomedical image segmentation. In International Conference on Medical image computing and computer-assisted intervention, pages 234–241. Springer, 2015.
[23] V. Sandfort, K. Yan, P. J. Pickhardt, and R. M. Summers. Data augmentation using generative adversarial networks (cyclegan) to improve generalizability in ct segmentation tasks. Scientific reports, 9(1):1–9, 2023.
[24] S. Sangeethaa and P. U. Maheswari. An intelligent model for blood vessel segmentation in diagnosing dr using cnn. Journal of medical systems, 42(10):175, 2018.
[25] T. Silva. An intuitive introduction to generative adversarial networks (gans). freeCodeCamp. org, 2018.
[26] C.L.Srinidhi,P.Aparna,andJ.Rajan.Recentadvancements in retinal vessel segmentation. Journal of medical systems, 41(4):70, 2017.
[27] J. Staal, M. D. Abra`moff, M. Niemeijer, M. A. Viergever, and B. Van Ginneken. Ridge-based vessel segmentation in color images of the retina. IEEE transactions on medical imaging, 23(4):501–509, 2004.
[28] K.Wisaeng,N.Hiransakolwong,andE.Pothiruk.Automatic detection of exudates in retinal images based on threshold moving average models. Biophysics, 60(2):288–297, 2015.
[29] H. Yazid, H. Arof, and H. M. Isa. Automated identification of exudates and optic disc based on inverse surface thresholding. Journal of medical systems, 36(3):1997–2004, 2012.
[30] H. Yu, E. S. Barriga, C. Agurto, S. Echegaray, M. S. Pattichis, W. Bauman, and P. Soliz. Fast localization and segmentation of optic disk in retinal images using directional matched filtering and level sets. IEEE Transactions on information technology in biomedicine, 16(4):644–657, 2012.
[31] L. Zhou, Q. Yu, X. Xu, Y. Gu, and J. Yang. Improving dense conditional random field for retinal vessel segmentation by discriminative feature learning and thin-vessel enhancement. Computer methods and programs in biomedicine, 148:13– 25, 2017.